HHS Public Access

Author manuscript

Bone. Author manuscript; available in PMC 2016 September 01.

Published in final edited form as:

Bone. 2015 September ; 78: 62–70. doi:10.1016/j.bone.2015.04.038.

Follistatin-like 3 is a mediator of exercise-driven bone formation and strengthening

J Nam[a], **P Perera**[b], **R Gordon**[b], **Y Jeong**[c], **AD Blazek**[d], **DG Kim**[c], **BC Tee**[c], **Z Sun**[c], **TD Eubank**[e], **Y Zhao**[f], **B Lablebecioglu**[g], **S Liu**[h], **A Litsky**[f], **NL Weisleder**[d], **BS Lee**[d], **T Butterfield**[i], **AL Schneyer**[j], and **S Agarwal**[b]

[a]Department of Bioengineering, University of California, Riverside, CA 92507

[b]Department of Biosciences, The Ohio State University, Columbus, OH 43210

[c]Department of Orthodontics, The Ohio State University, Columbus, OH 43210

[d]Department of Physiology and Cell Biology, The Ohio State University, Columbus, OH 43210

[e]Department of Internal Medicine, The Ohio State University, Columbus, OH 43210

[f]Department of Biomedical Engineering, The Ohio State University, Columbus, OH 43210

[g]Department of Periodontics, The Ohio State University, Columbus, OH 43210

[h]Hormel Institute, University of Minnesota, MN 55901

[i]Department of Physiology, University of Kentucky, Lexington, KY 40536

[j]Department of Veterinary and Animal Science, University of Massachusetts-Amherst, MA 01003

Abstract

Exercise is vital for maintaining bone strength and architecture. Follistatin like 3 (FSTL3), a member of Follistatin family, is a mechanosensitive protein upregulated in response to exercise and is involved in regulating musculoskeletal health, we investigated the potential role of FSTL3 in exercise-driven bone remodeling. Exercise-dependent regulation of bone structure and functions was compared in mice with global *Fstl3* gene deletion (*Fstl3*−/−) and their age-matched *Fstl3*+/+ littermates. Mice were exercised by low-intensity treadmill walking. The mechanical properties and mineralization were determined by μCT, three-point bending test and sequential incorporation of calcein and alizarin complexone. ELISA, Western-blot analysis and qRT-PCR were used to analyze the regulation of FSTL3 and associated molecules in the serum specimens and tissues. Daily exercise significantly increased circulating FSTL3 levels in mice, rats and humans. Compared to age-matched littermates, *Fstl3*−/− mice exhibited significantly lower fracture tolerance, having greater stiffness, but lower strain at fracture and yield energy. Furthermore,

Address correspondence to: Jin Nam, Ph.D., Department of Bioengineering, University of California-Riverside, Materials Science & Engineering Building 331, 900 University Avenue, Riverside, CA, 92521, jnam@engr.ucr.edu, TEL: 951-827-2064, FAX: 951-827-6416.

increased levels of circulating FSTL3 in young mice paralleled greater strain at fracture compared to the lower levels of FSTL3 in older mice. More significantly, *Fstl3*−/− mice exhibited loss of mechanosensitivity and irresponsiveness to exercise-dependent bone formation as compared to their *Fstl3*+/+ littermates. In addition, FSTL3 gene deletion resulted in loss of exercise-dependent sclerostin regulation in osteocytes and osteoblasts, as compared to *Fstl3*+/+ osteocytes and osteoblasts, *in vivo* and *in vitro*. The data identifies FSTL3 as a critical mediator of exercise-dependent bone formation and strengthening and point to its potential role in bone health and in musculoskeletal diseases.

Keywords

Follistatin-like 3; exercise; bone remodeling; osteoblast; osteocyte

1. Introduction

Exercise is a fundamental requirement for the maintenance of skeletal architecture and strength (1–3). Lack of mechanical loading/physical activity leads to bone loss frequently observed in aging, paraplegics, astronauts, and bone disorders, underscoring the importance of exercise in bone health (4–6). However, the underlying molecular targets that control exercise-driven bone formation remain less defined. To maintain skeletal strength and architecture, mechanical signals generated by exercise support an intricate balance between bone formation by osteoblasts and osteocytes and bone resorption by osteoclasts, under distinct but interdependent molecular control mechanisms (1, 2, 4). Osteoblasts and osteocytes are mechanosensitive and can perceive and respond to changes in their mechanical microenvironment. In response to appropriate levels of mechanical forces, these cells regulate Wnt signaling, bone morphogenic proteins (BMPs), hormones, and transcription factors (RUNX2 and OSX) critical for osteogenesis (6–10). The endogenous molecules are required for the complex regulation of recruitment and differentiation of bone cells through endocrine, paracrine, and autocrine mechanisms (6, 7).

Exercise upregulates the induction of the follistatin family of proteins in humans, including follistatin (FST), follistatin-like 1 (FSTL1) and follistatin-like 3 (FSTL3) (11–13). FST and FSTL3 bind and alter activities of the transforming growth factor-β (TGF-β) family of molecules such as activins, inhibins and myostatin to neutralize their functional activity, suggesting their role in many tissues including muscle regeneration (14, 15). Although originally identified in reproductive tissues, follistatins are produced by many different cell types and are present in the serum (16). The physiological significance of these proteins in skeletal development is highlighted by the severity of bone defects caused by *Fst* and *Fstl1* gene disruption in mice, which results in perinatal death, and poorly formed skeleton and musculature (17, 18). Recently, we observed that genomic disruption of *Fstl3* results in smaller skeletons in newborns, but no obvious skeletal deformities.

FSTL3 is a highly conserved 27–39 kDa monomeric glycoprotein (19). It is structurally and functionally distinct from the other follistatin family member, FST, as it contains only two follistatin domains and is present in the nucleus in a glycosylated form (16). Its role in suppressing osteoclast differentiation via binding to ADAM12 (a disintegrin and

metalloproteinase-12), modulating insulin sensitivity and fat homeostasis, and binding to BMPs suggest its likely role in bone metabolism (14, 20–22). Based on above observations and the exercise-driven upregulation of FSTL3, we examined its potential role in post-natal exercise-driven bone formation *in vivo* (10, 23), and verified the results in osteoblasts *in vitro*. Our findings provide the evidence that FSTL3 is a critical mediator of the exercise-driven bone formation and strengthening and likely acts upstream of Wnt signaling to induce osteogenesis.

2. METHODS

2.1. Animal and human studies

The Institutional Animal Care and Use Committee and Institutional Review Board at The Ohio State University preapproved all protocols prior to use of animals and human experiments. Skeletally mature Sprague Dawley rats (14–16 weeks old, females, n=10/group) and C57Bl/6 mice (12–14 weeks, females/males, n=10/group) were obtained from Charles River Laboratories (MA). Homozygous *Fstl3*−/− mice with global *Fstl3* gene deletion and their *Fstl3*+/+ littermates (12–14 weeks old females, unless otherwise indicated; n=5/group) were generated as described earlier (22). Healthy, non-habitually exercising human subjects were recruited for the study. Exercise regimens comprised of gentle treadmill walking for mice (8 m/min, 45 min/d), rats (12 m/min, 45 min/d), healthy 22–35 yrs old human subjects (3 miles/h, 45 min/d) and 68–74 years old human subjects (2–3 miles per h, 30–40 min/d) (24). All animals were allowed normal cage activity during the remaining time, along with non-exercised Controls. All animals were sacrificed 4 hours after the last exercise regimen to harvest blood and tissues. Blood was drawn from human subjects 6 h after exercise.

2.2. Assessment of mineral apposition rate (MAR)

MAR was assessed in the femurs of *Fstl3* +/+, homozygous *Fstl3* −/− mice, and heterozygous *Fstl3* +/− mice by the incorporation of fluorochromes via intraperitoneal injections of calcein (5mg/kg body weight) on day 3 and alizarin complexone (25 mg/kg body weight) on day 12 of the exercise regimens (25). The femurs were harvested on day 15, fixed in 10% neutralized formalin, dehydrated, and embedded in Micro-bed resin (Electron Microscopy Sciences, PA). Longitudinal or transverse sections of bones (30 μm thick) were examined under Zeiss epifluorescence microscope. The MAR was calculated as average distance between the centers of the two labels divided by the time interval between the two fluorochrome injections (26).

2.3. Quantitative measurements of the geometric properties of bones

Femurs of mice (n=5/group) were scanned by μCT (SkyScan 1172-D, Kontich, Belgium) with the scanning and reconstruction voxel sizes set at 20×20×20 μm^3. The same scanning conditions (49 kV, 200 μA, 0.4° rotation per projection and 8 frames averaged per projection) were used for all specimens. The CT attenuation value of each bone voxel (tissue mineral density, TMD) of bone was obtained, while bone voxels were segmented from non-bone voxels using the heuristic algorithm as described earlier (27). A 1 mm region at 55% of femoral length from the proximal end was dissected from the μCT images to be analyzed by

Image J software (NIH) (28). The mean TMD value was computed by dividing the sum of TMD values by the total number of voxels in each region using the TMD histograms. The variability of TMD was assessed by the coefficient of variation (COV) that was computed by dividing standard deviation by mean value of TMD. Anterioposterior to mediolateral size ratio (AP/ML) and moment of inertia of femurs were measured using a BoneJ plug-in function of the ImageJ for the section of femoral μCT image as described earlier (28–30).

2.4. Mechanical properties of bones

After μCT imaging, femurs (n=10) were subjected to three-point bending test (Bose Endura 3200 Tech System, MA) consisting of a custom-made fixture with a span length of 5 mm between the two base supports and load was applied to the mid-diaphysis on the anterior surface at a displacement rate of 0.5 mm/sec up to fracture. Subsequently, the stiffness, yield strain and energy, and strain at fracture were measured using load-displacement curves of the fracture testing (30, 31).

2.5. Primary osteoblast culture and exposure to dynamic compressive strain (DCS)

Calvarial osteoblasts were isolated from 4–5 day-old mice, cultured in PCL scaffolds and subjected to DCS (10% compression at 1 Hz) for required time as described earlier (32).

2.6. Quantitative reverse transcriptase polymerase chain reaction (qRT-PCR)

Bones were harvested, 2 mm^3 volume of bone just below the growth plate was split into smaller pieces and thoroughly washed with cold PBS to dislodge most of the non-adherent cells. Bone pieces were then pulverized in a Mikrodismembrator (Sartorius, GMBH) and RNA was extracted from primarily cortical bone and lining cells. Expression of mRNA was analyzed by qRT-PCR as previously described (33). The expression of the experimental target gene was normalized to a housekeeping gene transcript (*Rps18*) relative to a calibrator (untreated control), and was given as the estimation of $2\wedge\Delta\Delta C_T$ (34). The primers used for rat genes were *Rps18*-5′GCGGCGGAAAATAGCCTTCG3′ and 3′-GGCCAGTGGTCTTGGTGTGCTG5′; *Fstl3*-5′-ACGTTACCTACATCTCGTCGTGTC-3′ and 3′-TCCTCCTCTGCTGGTACTTTGG-5′; *Inha*-5′-CTTGTCCTGGCCAAAGTGAAG-3′ and 3′-TGGTTCAGAGGTCCTGTGCAT-5′; *Inhba*-5′-TAGAGGACGACATTGGCAGGA-3′ and 3′-TCGGCAAAGGTGATGATCTCC-5′; *Inhbb*-5′-GCAGACATCGCATCCGAAAA-3′ and 3′-AATGATCCAGTCGTTCCAGCC-5′; *Fst*-5′-GCTCCTCAAGGCCAGATGTAA-3′ and 3′-GCCTGGACAGAAAACATCCCT-5′; Mouse primers were *Rps18*-5′-GGAAAATAGCCTTCGCCATCACT-3′ and 3′-GCCAGTGGTCTTGGTGTGCTGAC-5′; *Fstl3*-5′-TTACCTACATCTCGTCGTGTCACCT-3′ and 3′-TCCTCCTCTGCTGGTACTTTGG-5′. The expression of mouse *Sost* (NM_024449.5) was carried out by Taqman Gene Expression Assays (Applied Biosystems).

2.7. Western blot analyses

Cellular proteins were extracted in RIPA buffer (Santa Cruz Biotechnology, CA) containing proteinase inhibitor (Roche Diagnostic, NJ). Prior to running gels, human and rat serum albumin were serum depleted by absorption on Cibachrome blue sepharose columns (Pierce,

IL). However, mouse serum albumin could not be completely depleted by similar technique. Equal concentrations of total protein and equal volume of serum were electrophoretically resolved on SDS-10% PAGE and transferred to a nitrocellulose membrane (Bio-Rad, CA), and probed with anti-rat/human or mouse biotinylated FSTL3 (R&D Systems, MN), sclerostin (Cell Signaling, MA) and anti-β-actin (Sigma, MO) primary antibodies. Secondary antibodies were IRDye 680 or IRDye 800 conjugated goat anti-rabbit or goat anti-mouse IgG (LI-COR, NE). The bands were digitized by for graphic presentations by LI-COR Odyssey imager and Odyssey application software, ver.2.1 (33). The FSTL3 bands for mouse serum were estimated by the location of a recombinant mouse FSTL3 (R&D Systems) band, and their protein identification was confirmed by mass spectroscopy.

2.8. Immunohistochemistry

IHC was carried out according to manufacturer's recommended protocol (R&D Systems, MN) on demineralized femoral sections using rabbit anti-FSTL3 or rabbit-anti SOST antibodies described above. Secondary antibodies were goat anti-rabbit IgG conjugated with HRP or TRITC (Cell Signaling, MA). To assess microcracks FSTL3−/− and FSTL3+/+ mice (18–22 mo old females) were injected with calcein intraperitoneally 3 days apart for 12 days. Subsequently, femurs were embedded in Micro-bed-resin and sections were cut at 20 μm thickness to quantify microcracks as described earlier (35, 36).

2.9. Statistical Analysis

All studies utilized 5 to 10 animals/group or 3–5 five replicates in *in vitro* experiments. Results are expressed as the mean ± standard error of the mean (SEM). Statistical analysis was performed using one-way ANOVA and a post hoc Tukey test using Minitab 14 Statistical Software. Results were considered statistically significant when $p < 0.05$.

3. RESULTS

Exercise upregulates FSTL3 expression in the circulation and musculoskeletal tissues

We first examined the exercise-dependent regulation of FSTL3 in the circulation (16). Western blot analysis revealed a significant upregulation of FSTL3 in rat, mouse and human sera in response to daily exercise for 2, 5 and 15 days, as compared to pre-exercise levels. Nevertheless, a slight decrease was observed on day 15 following daily exercise (Figures 1a–c).

We next examined the source of tissue responsible for FSTL3 upregulation in the serum (16). C57BL/6 adult female mice were subjected to daily exercise for 0 or 2 days and the expression of *Fstl3* in tissues was analyzed by qRT-PCR. As compared to non-exercised mice, a significant upregulation of *Fstl3* mRNA expression was mainly observed in musculoskeletal tissues, *i.e.*, bone, cartilage, vastus lateralis muscle, and anterior cruciate ligament, whereas its regulation was minimal in brown fat, liver, testes, ovaries, spleen and kidney (Figure 1d).

Exercise upregulates FSTL3 expression in osteocytes and osteoblasts *in vivo* and *in vitro*

Above results prompted us to analyze the transcript levels of *Fstl3* and its ligands in bone. Sprague-Dawley rats were subjected to a single regimen of exercise and the *Fstl3* mRNA expression was assessed at various time intervals. Gene expression analysis revealed that *Fstl3* mRNA was transiently upregulated within two hours and subsides to baseline by 24 h (Figure 2a). Furthermore, daily exercise for 0, 2, or 5 days resulted in upregulation of *Fstl3* mRNA expression, reaching approximately 6-fold increase by day 2 that subsequently decreased by day 5. In addition, *Fst* mRNA levels also significantly increased on day 2 and 5, while the mRNA expression of FSTL3 ligands inhibin-α (*Inha*), -βa (*Inhba*), and -βb (*Inhbb*) were not changed (Figure 2b). Immunohistochemistry revealed that FSTL3 expression was localized mainly in nuclei of the osteocytes and osteoblasts lining the bone in the sagittal sections of non-exercised rat femurs. However, a robust increase in FSTL3 expression was observed on day 2 and day 5 post exercise, predominantly in cells within or adjacent to bones (Figure 2cA–C). Osteocalcin staining of adjacent sections of the same bones revealed that FSTL3 positive cells were also osteocalcin positive, confirming the osteoblastic phenotype of these cells (Figures 2c, E–G). Control sections treated with secondary antibody alone did not exhibit FSTL3 (Figure 2c, D) or osteocalcin staining (Figure 2c, H). These results are consistent with bone matrix synthesis previously reported between 2 and 4 days following the onset of exercise regimens (37). We next confirmed that FSTL3 induction by mechanoactivation occurs in osteoblasts *in vitro*. Exposure of rat calvarial osteoblasts grown on 3–D polycaprolactone (PCL) microfiber scaffolds (32) to DCS (10% at 0.5 Hz) also exhibited a rapid and transient upregulation of *Fstl3* mRNA (Figure 2d) and protein expression (Figure 2e).

FSTL3 is required for bone strengthening

Since exercise induced upregulation of FSTL3 in osteocytes and osteoblasts, we next focused on its function in bone utilizing mice with global *Fstl3* gene deletion (22). Comparison of the newborn skeleton of *Fstl3*−/− mice with their *Fstl3*+/+ littermates revealed that the skeleton of *Fstl3*−/− mice were morphologically normal, but the relative size of skeletons at birth were 15% ± 6% smaller than *Fstl3*+/+ newborns (Figure 3a). Albeit this initial difference in size, femur length at 3 weeks of age were similar having 12.4 mm ± 0.2 for *Fstl3*+/+ and 12.1 ± 0.7 mm for *Fstl3*−/− (Figure 3b). Interestingly, anterioposterior and mediolateral ratios (AP/ML; 0.78±0.01 *vs* 0.69±0.04 for *Fstl3*−/− *vs* *Fstl3*+/+ mice, respectively) by μCT revealed that the mid shafts of *Fstl3*−/− femurs were more symmetrical as compared to *Fstl3*+/+ mice that were more anisotropic in shape (Figures 3c, d).

Since biomechanical strength of bones is critically regulated by exercise-induced bone remodeling, we next compared the mechanical properties of femurs from *Fstl3*−/− and *Fstl3*+/+ mice. The *Fstl3*−/− femurs showed significantly higher stiffness (163.8±30.9 *vs* 82.7±29.6 N/mm, $p < 0.05$) and moment of inertia (0.114±0.2 *vs* 0.087±0.2 mm^4, $p < 0.03$) than *Fstl3*+/+ mouse femurs (Figures 3e, f). In contrast, *Fstl3*−/− femurs had significantly lower strain at fracture of (0.014±0.006 *v*s 0.021±0.001 N/mm, $p < 0.05$) and yield energy (0.39±0.2 *vs* 0.69±0.1 MPa, $p < 0.05$) than the *Fstl3*+/+ mouse femurs (Figures 3g, h). The representative stress-strain curves of the cortical bones of the *Fstl3*+/+ and *Fstl3*−/−femurs

under three point bending test revealed that the strain at fracture of femurs from *Fstl3*+/+ mice was greater than that of *Fstl3*−/− mice (Figure 3i). These data show that the lack of FSTL3 results in stiffer and more brittle bones, indicating that FSTL3 mediates bone resilience and toughness, and that loss of FSTL3 results in bones that are more susceptible to breakage in a fall. The *Fstl3*−/− group also displayed a higher mean value of gray-levels than the *Fstl*+/+ littermates (123.6±10.7 *vs* 107.0±6.3, $p < 0.005$). Furthermore, the variability of gray levels in the *Fstl3*−/− group was significantly lower (0.15±0.009 *vs* 0.17±0.01, $p < 0.03$) than that in *Fstl3*+/+ group (Figure 3j), supporting the mechanical data that show the greater fragility of bones in *Fstl3*−/− mice.

Circulating FSTL3 levels are associated with bone strength

Comparisons of circulating FSTL3 levels were significantly greater in young mice (age 3–3.5 months) that those from older mice (age 18–22 months) (Figure 4a). Furthermore, circulating FSTL3 levels increased following 7 days of daily exercise, and it was significantly greater in young mice than in older mice. The differences in FSTL3 serum levels were paralleled by fracture strain of femurs from young mice (Figure 4b). The strain at fracture in *Fstl3*−/− mice was lower than *Fstl3*+/+ mice and remained relatively same in young and older mice (Figure 4c).

Bone microdamage is defined as damage to matrix visualized microscopically (35, 36). Microcracks are apparent in bones with deterioration of their biomechanical integriry. Therefore, to examine the consequences of the loss of bone strength in *Fstl3*−/− mice, we next determined the relative numbers of microcracks in bones of 18–22 months old female *Fstl3*−/− mice and compared to those from *Fstl3*+/+ mice. Incorporation of calcein followed by sectioning of mineralized bone revealed greater number of microcrackes in the femurs of older *Fstl3*−/− mice (mean number 108.0 ± 23/1000^2 μm; mean length 62.3± 13 μm) as compared to *Fstl3*+/+ mice (47.6± 12/1000^2 μm; mean length 32.3± 17 μm; Figure 4d). Interestingly, circulating levels of FSTL3 in the younger human subjects (age 22–35 yrs) were significantly greater than those from older adults (age 68–74 yrs) (Figure 4e).

FSTL3 is required for exercise-driven bone formation

Since above experiments demonstrated that loss of FSTL3 results in weaker/brittle bones, we also postulated its involvement in exercise-dependent bone remodeling. Female *Fstl3*−/− and *Fstl3*+/+ mice were subjected to daily exercise for 15 days. Following incorporation of fluorochromes calcein and alizarin complexone on days 3 and 10 repectively, the mineral apposition in the cortical bone closer to distal ends of femurs was examined in cross-sections (Figures 5a, c) and in the mid-shaft region in longitudinal sections of the femurs (Figure 5b). *Fstl3*+/+ mice exhibited some constitutive bone deposition in non-exercised controls, and exercise-induced significant bone deposition at the endosteal side than at the periosteal side of the cortical bone (Figures 5a–c). Contrarily, some constitutive bone deposition was apparent in *Fstl3*−/− mice, but it was unchanged in response to exercise (Figures 5a–c). We also observed gain of partial mechanoresponsiveness in *Fstl3*+/− *mice* as apparent by increase in the distance between calcein and alizarin bands, further confirming a role for FSTL3 in exercise-dependent bone formation (Figure 5a, c). The loss of mechanoresponsiveness was observed in both male and female *Fstl3*−/− mice, as

compared to their *Fstl3*+/+ littermates (Figure 5b). The significantly greater MAR confirmed that exercise-dependent mineral deposition occurred at the endosteal surface of the cortical bone in *Fstl3*+/+ and *Fstl3*+/− mice, but not in *Fstl3*−/− mice (Figure 5c). Interestingly, we did not see a significant increase in the MAR on the periosteal surface of the bone in response to exercise during the first 15 days (Figure 5d). Histological analysis of the vertical sections of femurs also exhibited osteoid formation at a number of endosteal sites in *Fstl3*+/+ mice, which were minimal in *Fstl3*−/− in spite of bone surfaces being covered by lining cells (Figure 5e).

It is important to note that both *Fstl3*+/+ and *Fstl*3−/− showed some degree of spontaneous bone formation in both non-exercised and exercised mice, at both endosteal and periosteal surfaces of the cortical bone (Figures 5a–d).

Presence of FSTL3 is critical for mechano-regulation of SOST

SOST has shown to inhibit bone formation via Wnt signaling (1, 38, 39). Therefore, regulation of SOST in *Fstl3*+/+ and *Fstl3*−/− mice was examined. Calvarial osteoblasts from *Fstl3*+/+ and *Fstl3*−/− mice were cultured on 3D-PCL scaffolds and subjected to DCS (10% at 0.5 Hz) for 2 h (32). qRT-PCR analysis showed a significant suppression of *Sost* mRNA in *Fstl3*+/+ osteoblasts 4 or 24 h later, but such downregulation was not observed in *Fstl3*−/− osteoblasts (Figure 6a). Similarly, constitutive protein levels of SOST in *Fstl3*+/+ osteoblasts were lower as compared to *Fstl3*−/− osteoblasts. Similar to the gene expression, SOST levels were unchanged following DCS exposure in *Fstl3*−/− osteoblasts, whereas a slight decrease in SOST by DCS was apparent in *Fstl3*+/+ osteoblasts (Figures 6b, c). We next determined the expression of SOST in osteocytes in the femurs of *Fstl3*−/− and *Fstl3*+/+ mice. Relative SOST intensity by immunohistochemistry showed that *Fstl3*+/+ mice expressed significantly lower SOST in osteocytes in cortical bone of femurs as compared to *Fstl3*−/− mice femurs. Furthermore, SOST expression in *Fstl3*−/− osteocytes was unchanged in response to exercise, following 2 and 5 days of exercise (Figures 6d, e).

4. DISCUSSION

Regular exercise is well known to upregulate bone strength and architecture, but the mediators of such regulation are less defined (1, 2, 26). While the follistatin family were shown to regulate muscle strengthening earlier (15, 40), present findings are the first to demonstrate a role of FSTL3 in exercise-driven bone formation and strengthening. *Fstl3* is an adaptive response gene regulated by exercise in many tissues, but particularly in bone and cartilage. A single session of moderate intensity walking induces *Fstl3* mRNA rapidly but transiently and drops to control levels within 24 h, suggesting that daily exercise may be necessary to maintain the levels of FSTL3 locally in bone and systemically in the serum. FSTL3 levels in circulation are also dramatically upregulated by exercise on day 2 and day 5 and remain greater than control levels following 15 days of daily exercise, suggesting its stringent control by exercise. Furthermore, the observed time course of FSTL3 expression in osteocalcin-positive osteocytes and osteoblasts in bone is in alignment with the time course of exercise-dependent osteoid formation observed earlier (38, 41). The upregulation of *Fstl3* mRNA and protein in calvarial osteoblasts by DCS further confirms that FSTL3 is a mechanosensitive protein produced in bone. The functional differences in circulating versus

local FSTL3 in bone are not yet clear. However, it is tempting to speculate that both circulating and local FSTL3 may be important for the exercise-driven systemic regulation of bone formation and strengthening.

Exercise strongly influences skeletal ossification and regulates changes in bone geometry and strength (1, 2, 39). This mechanoresponsiveness of bone is apparent by strain-dependent anisotropic bone remodeling, consequent changes in bone architecture and increased bone strength (27, 42). In particular, we found that *Fstl3*−/− femurs have more homogeneous tissue mineral distribution and less viscoelastic properties, resulting in increase in tissue brittleness, microcracks of bone, more symmetric/roundish bone cross sections, and dramatically reduced bone strength than those from *Fstl3*+/+ littermates. Together, these findings support that FSTL3 is a critical regulator of cellular adaptation to mechanical forces in bones and modulates not only bone mineralization, but also consequent viscoelastic properties, brittleness and bone strengthening.

Another finding that provides experimental support for a causal relationship between FSTL3 and bone strengthening comes from the observed higher circulating FSTL3 levels, which are paralleled by greater fracture strain in the femurs of young *Fstl3*+/+ mice (age 3–3.5 months). In contrast, lower circulating levels of FSTL3 are paralleled by lower fracture strain in the femurs of older (age 20–22 months) mice. Similarly in aging humans, lower levels of circulating FSTL3 parallel lower bone mineral density assessed by dual-energy x-ray absorptiometry (DXA). Interestingly, these findings correlate the epidemiological outcomes that chronic lack of mechanical loading or sedentary lifestyle in the elderly leads to bone loss, whereas exercise prevents bone loss and strengthens bones (2, 4, 43). In this context, the lower levels of FSTL3 in elderly subjects further suggest that the levels of circulating FSTL3 may be essential for sustaining strong bones systemically and its low levels in circulation could potentially serve as an indicator for bone loss.

In parallel to bone strengthening, our studies demonstrate that FSTL3 is a critical mediator of exercise-dependent bone formation. The observations from histofluorometric studies show that *Fstl3*−/− mice failed to deposit bone in response to exercise, which could be partially reconstituted in the heterozygous *Fstl3*+/− mice. This strongly suggests that exercise-driven bone formation requires FSTL3. Interestingly, Fstl3−/− mice, by 3–4 weeks of age, have similar size and shape of bones as their age-matched littermates, possibly suggesting that slow constitutive (non-exercise-driven) bone deposition on all sides of femurs in *Fstl3*−/− mice is likely regulated by non-mechanosensitive mediators of bone formation. The intrinsically stiffer bones in *Fstl3*−/− mice could have partly contributed to the non-mechanoresponsiveness by reducing the magnitudes of strain which is experienced by bone cells under the same load as compared to those in wild type mice. However, the fact that the bone cells isolated from *Fstl3*−/− mice were irresponsive to DCS in the *in vitro* experiments, strongly suggests that the loss of FSTL3 results in the mechano-insensitivity of bone cells.

Mechanical signals are critical for the cellular differentiation and functional maturation of osteocytes/osteoblasts required for bone formation. This activation of osteoblasts by mechanical signals is mediated via Wnt signaling cascade, where SOST acts as a

mechanosensitive inhibitor of Wnt signaling to suppress bone formation (1, 44). We showed that DCS in *Fstl3*+/+ but not in *Fstl3*−/− osteoblasts, significantly suppresses *Sost* mRNA induction and protein synthesis *in vitro*. Further, minimal expression of SOST in osteocytes from *Fstl3*+/+ femurs, its suppression after 2 or 5 days of exercise, and 2.5–3 fold greater constitutive expression in *Fstl3*−/− mice collectively suggest that FSTL3 may likely act upstream of SOST signaling cascade. Presently, it is unclear how mechanical signals are perceived by cells to bring about activation of diverse signaling pathways. It is likely that mechanical forces activate many receptors simultaneously via a common mechanism such as cell-matrix adhesion complexes that form physical link between extracellular matrix and cytoskeleton (45).

Our findings that FSTL3, a reproductive system associated protein, also regulates bone formation, fits well into the established literature, as ample research demonstrates that molecules produced by reproductive organs may play a role in bone formation and *vice versa*. For example, both estrogens and androgens are major regulators of bone formation, and their deficiency is associated with bone loss (7, 46). Similarly, osteocalcin, predominantly a bone protein, regulates optimal male fertility in mice and humans via the testosterone-pancreas-bone axis (47–49). Furthermore, overexpression of FSTL3 has been recently shown to induce increased insulin sensitivity (50). Thus, FSTL3 provides another example of a molecule associated with gonadal development that can regulate bone formation in an exercise-dependent manner. In fact, all follistatin family members thus far tested, FST, FSTL3 and FSTL1, are mechanosensitive proteins. The role of FST and FSTL1 in bone formation is as yet unclear; nevertheless, gene deletion studies show that FST and FSTL1 are associated with embryonic bone and muscle formation (40, 51). Given the fact that the protein structure of FSTL3 shares about 80% homology to FST, it would not be surprising if multiple follistatin members are involved in mechanotransduction and regulation of overall load-dependent bone formation (11–13). Intriguingly, while the FSTL3 molecule is devoid of heparin binding sites, it takes an active part in many cellular processes, i.e., it inhibits osteoclast differentiation and activation *in vitro*, improves insulin sensitivity, and regulates osteoclast differentiation via binding to ADAM12 (21). These observations suggest that FSTL3 may activate cells by associating with a specific receptor or via binding to other proteins (21).

Overall, present observations provide novel evidence that *Fstl3*, a rapid response gene, is a mediator of exercise-driven bone formation and strengthening. Exercise upregulates *Fstl3* mRNA and protein expression in osteoblasts. FSTL3 gene deletion results in loss of mechanosensitivity, bone mechanical strength and exercise driven bone formation, paralleled by loss of SOST regulation. Interestingly, exercise regulates bone and muscle structure and strength simultaneously in an integrated manner (52). FSTL3 is also shown to regulate muscle mass by neutralizing myostatin, an inhibitor of muscle growth that is downregulated by exercise (40, 51). It is yet to be seen, whether exercise-driven upregulation of muscle formation coordinates the integrated bone formation and strengthening simultaneously with muscle strengthening (40). Importantly, the marked but transient upregulation of FSTL3 in the serum of exercising humans provides a unique platform for analyzing the effects of exercise on bone health as yet not feasible by analysis

of other serum markers. Since FSTL3 appears to be a stringently controlled molecule, its expression levels could also provide an indicator for measuring the effects of exercise necessary for optimal bone formation in healthy adults, elderly, and in patients suffering from metabolic bone disorders.

Acknowledgments

This work was supported by Grant numbers AR048781 (S.A.) from the National Institute of Arthritis Musculoskeletal and Skin Diseases, and DE015399 (S.A.) and T32DE014320 (R.G.) from the National Institute of Dental and Craniofacial Research at the National Institute of Health, Bethesda, MD. This work was also partly supported by UCR initial complement funding (J.N.).

References

1. Turner CH, Warden SJ, Bellido T, Plotkin LI, Kumar N, Jasiuk I, et al. Mechanobiology of the skeleton. Sci Signal. 2009 Apr 28.2(68):pt3. [PubMed: 19401590]
2. Robling AG, Turner CH. Mechanical signaling for bone modeling and remodeling. Crit Rev Eukaryot Gene Expr. 2009; 19(4):319–38. [PubMed: 19817708]
3. Bone up on bone health. A practical guide to preserving your bone density. Mayo Clin Health Lett. 2011 Feb.(Suppl):1–8.
4. Knapik DM, Perera P, Nam J, Blazek AD, Rath B, Leblebicioglu B, et al. Mechanosignaling in Bone Health, Trauma and Inflammation. Antioxid Redox Signal. 2013 Aug 12.
5. Rath B, Nam J, Deschner J, Schaumburger J, Tingart M, Grassel S, et al. Biomechanical forces exert anabolic effects on osteoblasts by activation of SMAD 1/5/8 through type 1 BMP receptor. Biorheology. 2011; 48(1):37–48. [PubMed: 21515935]
6. Ozcivici E, Luu YK, Adler B, Qin YX, Rubin J, Judex S, et al. Mechanical signals as anabolic agents in bone. Nat Rev Rheumatol. 2010 Jan; 6(1):50–9. [PubMed: 20046206]
7. Frenkel B, Hong A, Baniwal SK, Coetzee GA, Ohlsson C, Khalid O, et al. Regulation of adult bone turnover by sex steroids. J Cell Physiol. 2010 Aug; 224(2):305–10. [PubMed: 20432458]
8. Bonewald LF. Osteocytes as dynamic multifunctional cells. Ann N Y Acad Sci. 2007 Nov. 1116:281–90. [PubMed: 17646259]
9. Nakashima K, Zhou X, Kunkel G, Zhang Z, Deng JM, Behringer RR, et al. The novel zinc finger-containing transcription factor osterix is required for osteoblast differentiation and bone formation. Cell. 2002 Jan 11; 108(1):17–29. [PubMed: 11792318]
10. Rath B, Nam J, Knobloch TJ, Lannutti JJ, Agarwal S. Compressive forces induce osteogenic gene expression in calvarial osteoblasts. J Biomech. 2008; 41(5):1095–103. [PubMed: 18191137]
11. Hansen J, Brandt C, Nielsen AR, Hojman P, Whitham M, Febbraio MA, et al. Exercise induces a marked increase in plasma follistatin: evidence that follistatin is a contraction-induced hepatokine. Endocrinology. 2011 Jan; 152(1):164–71. [PubMed: 21068158]
12. Gorgens SW, Raschke S, Holven KB, Jensen J, Eckardt K, Eckel J. Regulation of follistatin-like protein 1 expression and secretion in primary human skeletal muscle cells. Arch Physiol Biochem. 2013 May; 119(2):75–80. [PubMed: 23419164]
13. Dalbo VJ, Roberts MD, Hassell S, Kerksick CM. Effects of pre-exercise feeding on serum hormone concentrations and biomarkers of myostatin and ubiquitin proteasome pathway activity. Eur J Nutr. 2013 Mar; 52(2):477–87. [PubMed: 22476926]
14. Sidis Y, Mukherjee A, Keutmann H, Delbaere A, Sadatsuki M, Schneyer A. Biological activity of follistatin isoforms and follistatin-like-3 is dependent on differential cell surface binding and specificity for activin, myostatin, and bone morphogenetic proteins. Endocrinology. 2006 Jul; 147(7):3586–97. [PubMed: 16627583]
15. Hill JJ, Davies MV, Pearson AA, Wang JH, Hewick RM, Wolfman NM, et al. The myostatin propeptide and the follistatin-related gene are inhibitory binding proteins of myostatin in normal serum. J Biol Chem. 2002 Oct 25; 277(43):40735–41. [PubMed: 12194980]

16. Tortoriello DV, Sidis Y, Holtzman DA, Holmes WE, Schneyer AL. Human follistatin-related protein: a structural homologue of follistatin with nuclear localization. Endocrinology. 2001 Aug; 142(8):3426–34. [PubMed: 11459787]
17. Matzuk MM, Lu N, Vogel H, Sellheyer K, Roop DR, Bradley A. Multiple defects and perinatal death in mice deficient in follistatin. Nature. 1995 Mar 23; 374(6520):360–3. [PubMed: 7885475]
18. Sylva M, Li VS, Buffing AA, van Es JH, van den Born M, van der Velden S, et al. The BMP antagonist follistatin-like 1 is required for skeletal and lung organogenesis. PLoS One. 2011; 6(8):e22616. [PubMed: 21826198]
19. Schneyer A, Tortoriello D, Sidis Y, Keutmann H, Matsuzaki T, Holmes W. Follistatin-related protein (FSRP): a new member of the follistatin gene family. Mol Cell Endocrinol. 2001 Jun 30; 180(1–2):33–8. [PubMed: 11451569]
20. Saito S, Sidis Y, Mukherjee A, Xia Y, Schneyer A. Differential biosynthesis and intracellular transport of follistatin isoforms and follistatin-like-3. Endocrinology. 2005 Dec; 146(12):5052–62. [PubMed: 16150905]
21. Bartholin L, Destaing O, Forissier S, Martel S, Maguer-Satta V, Jurdic P, et al. FLRG, a new ADAM12-associated protein, modulates osteoclast differentiation. Biol Cell. 2005 Jul; 97(7):577–88. [PubMed: 15574124]
22. Mukherjee A, Sidis Y, Mahan A, Raher MJ, Xia Y, Rosen ED, et al. FSTL3 deletion reveals roles for TGF-beta family ligands in glucose and fat homeostasis in adults. Proc Natl Acad Sci U S A. 2007 Jan 23; 104(4):1348–53. [PubMed: 17229845]
23. Thompson WR, Rubin CT, Rubin J. Mechanical regulation of signaling pathways in bone. Gene. 2012 Jul 25; 503(2):179–93. [PubMed: 22575727]
24. Nam J, Perera P, Liu J, Wu LC, Rath B, Butterfield TA, et al. Transcriptome-wide gene regulation by gentle treadmill walking during the progression of monoiodoacetate-induced arthritis. Arthritis Rheum. 2011 Jun; 63(6):1613–25. [PubMed: 21400474]
25. Javaheri B, Stern AR, Lara N, Dallas M, Zhao H, Liu Y, et al. Deletion of a single beta-catenin allele in osteocytes abolishes the bone anabolic response to loading. J Bone Miner Res. 2014 Mar; 29(3):705–15. [PubMed: 23929793]
26. Turner CH, Robling AG. Exercise as an anabolic stimulus for bone. Curr Pharm Des. 2004; 10(21):2629–41. [PubMed: 15320750]
27. Kim DG, Navalgund AR, Tee BC, Noble GJ, Hart RT, Lee HR. Increased variability of bone tissue mineral density resulting from estrogen deficiency influences creep behavior in a rat vertebral body. Bone. 2012 Nov; 51(5):868–75. [PubMed: 22944606]
28. Doube M, Klosowski MM, Arganda-Carreras I, Cordelieres FP, Dougherty RP, Jackson JS, et al. BoneJ: Free and extensible bone image analysis in ImageJ. Bone. 2010 Dec; 47(6):1076–9. [PubMed: 20817052]
29. Kim DG, Christopherson GT, Dong XN, Fyhrie DP, Yeni YN. The effect of microcomputed tomography scanning and reconstruction voxel size on the accuracy of stereological measurements in human cancellous bone. Bone. 2004 Dec; 35(6):1375–82. [PubMed: 15589219]
30. Kim DG, Shertok D, Ching Tee B, Yeni YN. Variability of tissue mineral density can determine physiological creep of human vertebral cancellous bone. J Biomech. 2011 Jun 3; 44(9):1660–5. [PubMed: 21481880]
31. Voide R, van Lenthe GH, Muller R. Bone morphometry strongly predicts cortical bone stiffness and strength, but not toughness, in inbred mouse models of high and low bone mass. J Bone Miner Res. 2008 Aug; 23(8):1194–203. [PubMed: 18348694]
32. Nam J, Perera P, Rath B, Agarwal S. Dynamic regulation of bone morphogenetic proteins in engineered osteochondral constructs by biomechanical stimulation. Tissue Eng Part A. 2013 Mar; 19(5–6):783–92. [PubMed: 23198877]
33. Nam J, Perera P, Liu J, Rath B, Deschner J, Gassner R, et al. Sequential alterations in catabolic and anabolic gene expression parallel pathological changes during progression of monoiodoacetate-induced arthritis. PLoS One. 2011; 6(9):e24320. [PubMed: 21931681]
34. Nam J, Perera P, Liu J, Rath B, Deschner J, Gassner R, et al. Sequential alterations in catabolic and anabolic gene expression parallel pathological changes during progression of monoiodoacetate-induced arthritis. PLoS ONE. 2011; 6(9):e24320. [PubMed: 21931681]

35. Lee TC, Myers ER, Hayes WC. Fluorescence-aided detection of microdamage in compact bone. J Anat. 1998 Aug; 193(Pt 2):179–84. [PubMed: 9827633]
36. Dai RC, Liao EY, Yang C, Wu XP, Jiang Y. Microcracks: an alternative index for evaluating bone biomechanical quality. J Bone Miner Metab. 2004; 22(3):215–23. [PubMed: 15108063]
37. Hsieh YF, Robling AG, Ambrosius WT, Burr DB, Turner CH. Mechanical loading of diaphyseal bone in vivo: the strain threshold for an osteogenic response varies with location. J Bone Miner Res. 2001 Dec; 16(12):2291–7. [PubMed: 11760844]
38. Robling AG, Niziolek PJ, Baldridge LA, Condon KW, Allen MR, Alam I, et al. Mechanical stimulation of bone in vivo reduces osteocyte expression of Sost/sclerostin. J Biol Chem. 2008 Feb 29; 283(9):5866–75. [PubMed: 18089564]
39. Robling AG, Castillo AB, Turner CH. Biomechanical and molecular regulation of bone remodeling. Annu Rev Biomed Eng. 2006; 8:455–98. [PubMed: 16834564]
40. Lee SJ, Lee YS, Zimmers TA, Soleimani A, Matzuk MM, Tsuchida K, et al. Regulation of muscle mass by follistatin and activins. Mol Endocrinol. 2010 Oct; 24(10):1998–2008. [PubMed: 20810712]
41. Turner CH, Robling AG. Mechanisms by which exercise improves bone strength. J Bone Miner Metab. 2005; 23(Suppl):16–22. [PubMed: 15984409]
42. Ettinger B, Burr DB, Ritchie RO. Proposed pathogenesis for atypical femoral fractures: lessons from materials research. Bone. 2013 Aug; 55(2):495–500. [PubMed: 23419776]
43. Booth FW, Roberts CK, Laye MJ. Lack of exercise is a major cause of chronic diseases. Compr Physiol. 2012 Apr; 2(2):1143–211. [PubMed: 23798298]
44. Chennimalai Kumar N, Dantzig JA, Jasiuk IM, Robling AG, Turner CH. Numerical modeling of long bone adaptation due to mechanical loading: correlation with experiments. Ann Biomed Eng. 2010 Mar; 38(3):594–604. [PubMed: 20013156]
45. Ingber DE. Cellular mechanotransduction: putting all the pieces together again. FASEB J. 2006 May; 20(7):811–27. [PubMed: 16675838]
46. Nicks KM, Fowler TW, Gaddy D. Reproductive hormones and bone. Curr Osteoporos Rep. 2010 Jun; 8(2):60–7. [PubMed: 20425612]
47. Oury F, Ferron M, Huizhen W, Confavreux C, Xu L, Lacombe J, et al. Osteocalcin regulates murine and human fertility through a pancreas-bone-testis axis. J Clin Invest. 2013 Jun 3; 123(6): 2421–33. [PubMed: 23728177]
48. Oury F, Sumara G, Sumara O, Ferron M, Chang H, Smith CE, et al. Endocrine regulation of male fertility by the skeleton. Cell. 2011 Mar 4; 144(5):796–809. [PubMed: 21333348]
49. Schuh-Huerta SM, Pera RA. Reproductive biology: bone returns the favour. Nature. 2011 Apr 7; 472(7341):46–7. [PubMed: 21475191]
50. Brandt C, Hansen RH, Hansen JB, Olsen CH, Galle P, Mandrup-Poulsen T, et al. Over-expression of Follistatin-like 3 attenuates fat accumulation and improves insulin sensitivity in mice. Metabolism. 2015 Feb; 64(2):283–95. [PubMed: 25456456]
51. Lee SJ, McPherron AC. Myostatin and the control of skeletal muscle mass. Curr Opin Genet Dev. 1999 Oct; 9(5):604–7. [PubMed: 10508689]
52. Robling AG. Muscle loss and bone loss: master and slave? Bone. 2010 Feb; 46(2):272–3. [PubMed: 20045499]

Highlights

- FSTL3 is upregulated in osteocytes and osteoblasts under mechanical loading.
- FSTL3 is associated with load-dependent bone formation and strengthening.
- FSTL3 gene ablation results in the loss of mechano-responsive bone remodeling.

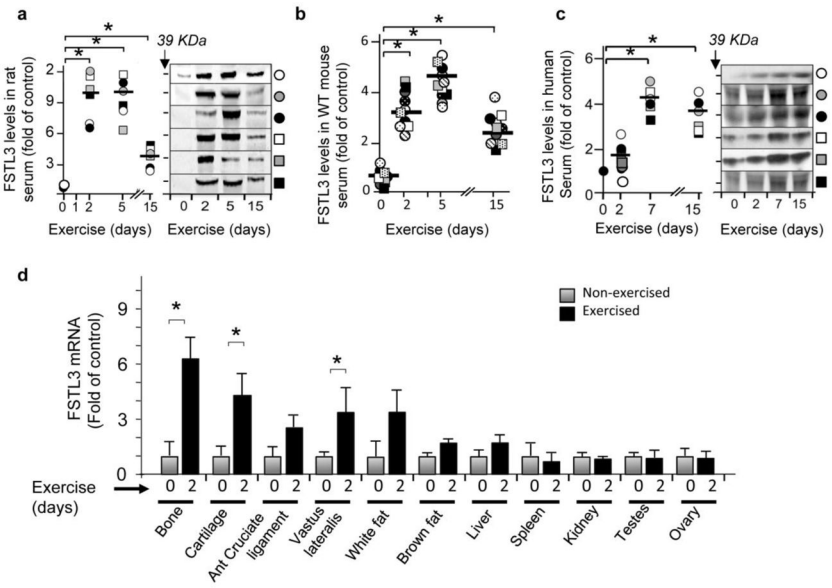

Figure 1. Exercise upregulates FSTL3 expression in circulation and tissues

Western blot analysis of serum specimens obtained from (**a**) rat, (**b**) mice, and (**c**) humans showing upregulation of FSTL3 following daily exercise from 0 to 15 days. Serum specimens were obtained 3 h following the last session of exercise from (a) rats (12 m/min for 45 min/day; 12–14 week old) and (b) mice (7 m/min for 45 min/day; 10–12 week old), and (c) following 6 h of the last session of exercise from human subjects (3 miles/h for 45 min/day; 20–35 years old males (circles) and females (squares)). Data represent SEM of at least 6 individual serum specimens in each case with a bar indicating the mean value. (**d**) Examination of FSTL3 expression in response to exercise in various tissues. Mice were exposed to daily exercise for 0 or 2 days, RNA was extracted from various tissues and *Fstl3* mRNA expression determined by qRT-PCR. Data represent mRNA analysis in duplicates from tissues of three mice/group at each time point. * represents $p < 0.05$.

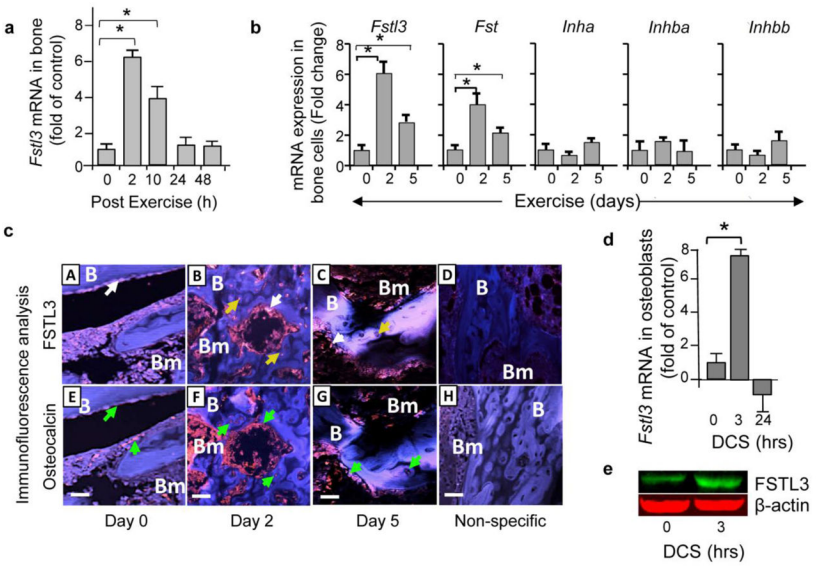

Figure 2. Exercise transiently upregulates FSTL3 expression in osteoblasts and osteocytes *in vivo* and *in vitro*

(a) Rats (n = 5/group) were exercised for 45 min and the Fstl3 mRNA expression examined following 2, 10, 24 or 48 h by qRT-PCR. (b) Rats (n = 10/group) were exercised daily for 0, 2, or 5 days. Bones were harvested 2 h after the last exercise regimen, and the expression of mRNA for *Fstl3, Fst,* inhibin(Inh)-α, Inh-βa and *Inh-βb* examined by qRT-PCR. (c) Immunofluorescence analysis of two adjacent sections of rat femurs showing exercise-dependent induction of FSTL3 (A–C) and the presence of osteocalcin (E–G) in areas immediately below growth plate, prior to exercise (A and E) or post-exercise on day 2 (B and F) or day 5 (C and G). The presence of FSTL3 in osteocytes is shown by yellow arrows and in bone lining cells by white arrows (A–C). The presence of osteocalcin is shown by green arrows (E–G). B, bone, Bm, bone marrow. Scale bar = 50 μm. (D and H) Sections stained with secondary antibodies alone showing no reactivity to cells. (d) Upregulation of *Fstl3* mRNA and (e) protein expression in calvarial osteoblasts in response to dynamic compressive strain *in vitro* (10% compression at 0.5 Hz). In all graphs, error bars indicate SEM, * $p < 0.05$.

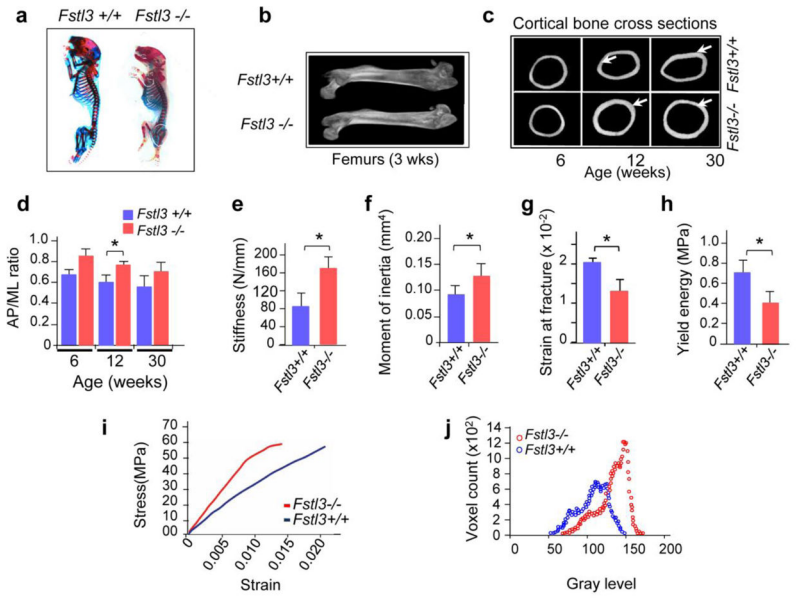

Figure 3. Loss of FSTL3 expression results in altered mechanical properties of bone

(**a**) Skeletons of newborn *Fstl3*+/+ and *Fstl3*−/− mice showing phenotypic similarities but differences in overall size. (**b**) μCT 3-D images of femurs from *Fstl3*+/+ and *Fstl3*−/− mice showing similar bone length by 3 weeks of age. (**c**) Analysis of bone architecture by μCT. Cross sections of mouse femurs at mid shaft at the ages of 6, 12 and 30 weeks, exhibiting the rounded shape of cortical bone in *Fstl3*−/− in comparison to anisotropic shape of *Fstl3*+/+ femurs. Quantification of (**d**) anterioposterior to mediolateral size ratio of femurs from *Fstl3*+/+ and *Fstl3*−/− mice, (**e**) bone stiffness, (**f**) moment of inertia, (**g**) strain at fracture and (**h**) yield energy in 12–14 week old *Fstl3*+/+ and *Fstl3*−/− mice. (**i**) Stress/strain graphs from *Fstl3*+/+ and *Fstl3*−/− mice show greater yield energy of femurs in *Fstl3*+/+ mice compared to *Fstl3*−/− mice. The graph is representative of ten replicates. (**j**) Typical gray-level density histograms of *Fstl3*+/+ and *Fstl3*−/− cortical bones from μCT imaging exhibiting greater variability in gray-levels in Fstl3+/+ mice. Error bars in all graphs indicate SEM, * $p < 0.05$.

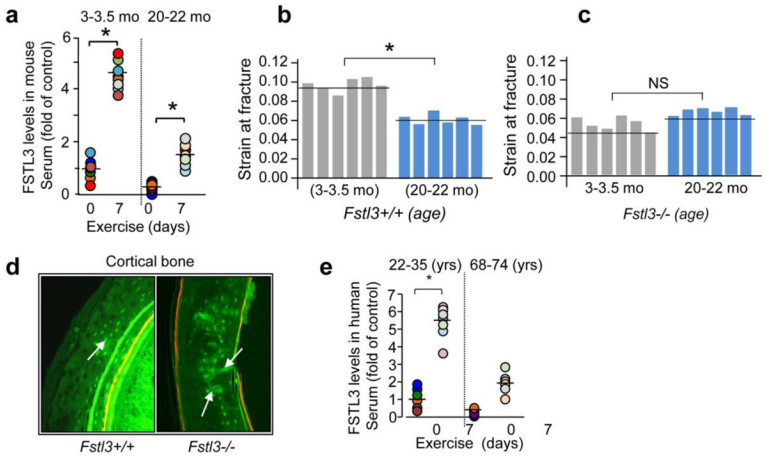

Figure 4. Age-dependent changes in circulating FSTL3 levels and fracture strain of femurs

(**a**) Serum FSTL3 levels from young (age 3–3.5 mo) and old (age 20–22 mo) *Fstl3*+/+ mice. (**b**) Strain at fracture of femurs from young (age 3–3.5 mo) and old (age 20–22 mo) *Fstl3*+/+ mice demonstrating age-dependent degradation while (**c**) Strain at fracture of femurs from young and old *Fstl3*−/− mice showing minimal age-dependent differences. (**d**) Cross sections of calcein labeled cortical bone from mid femurs of *Fstl3*+/+ and *Fstl3*−/− mice at 18–22 mo of age, showing increased number of microcracks in *Fstl3*−/− femurs. (**e**) Serum FSTL3 levels in young (age 22–35 yrs) and old (age 70–82 yrs) human subjects pre- and post- 7 days of exercise. * indicates $p < 0.05$.

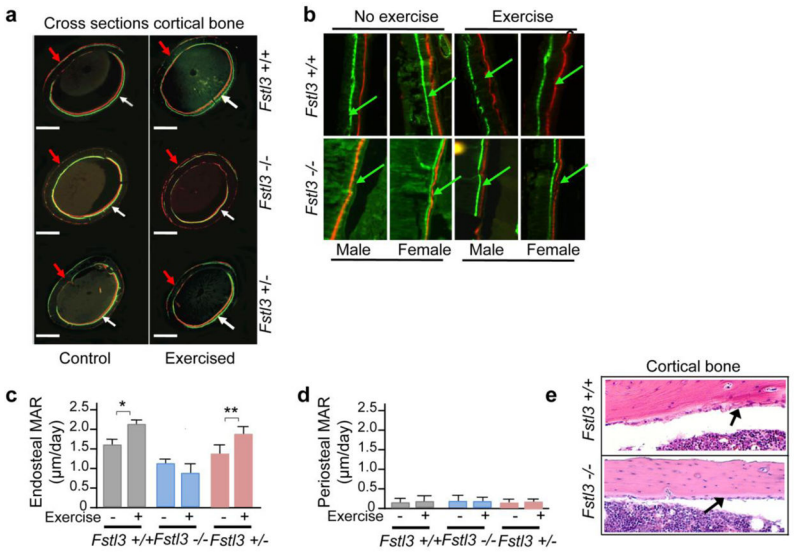

Figure 5. *Fstl3* gene deletion results in the loss of exercise-driven bone formation

Mice were exercised daily, intraperitoneally injected Calcein on day 3 and Alizarin complexone on day 12, and femurs harvested on day 15. (**a**) The transverse sections of femurs showing minimal bone formation, based on separation between calcein (green) and alizarin (red) incorporation, from non-exercised *Fstl3*+/+, *Fstl3*−/− and *Fstl3*+/− mice. Exercise induced greater bone deposition in *Fstl3*+/+ mice and *Fstl3*+/− *mice*, but not in *Fstl3*−/− mice. White arrows indicate changes in Calcein and Alizarin incorporation over 10 days on the endosteal surface, and red arrows show changes on the periosteal surface. Scale bar = 500 μM. (**b**) The sagittal sections of cortical bone from *Fstl3*+/+ and *Fstl3*−/− mice showing no differences in exercise-dependent bone formation between males and females. (**c**) Quantification of mineral apposition rate (MAR) in *Fstl3*+/+, *Fstl3*−/− and *Fstl3*+/− mice (n=8/group) based on Calcein and Alizarin incorporation at the endosteal surface and (**d**) at the periosteal surface. (**e**) H&E stained sagittal sections of femurs from 12 week old mice exercised for 2 weeks, demonstrating osteoid formation (arrows) in *Fstl3*+/+ mice, but minimal osteoid formation in *Fstl3*−/− mice. Scale bars = 150 μm.

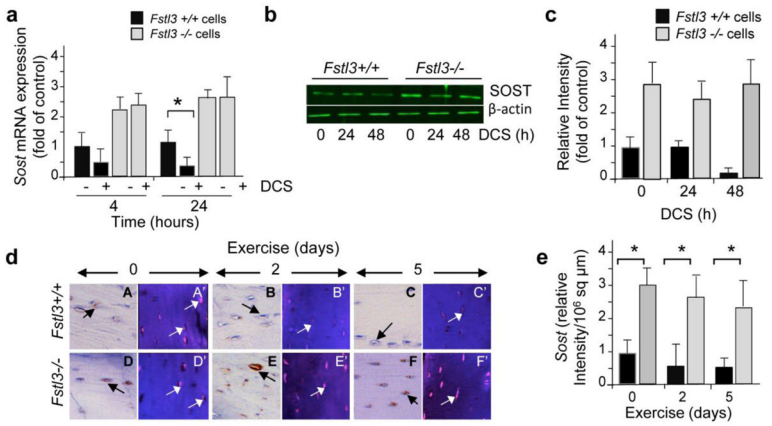

Figure 6. Exercise-dependent regulation of bone formation by FSTL3 is paralleled by *Sost* expression

(**a**) Calvarial osteoblasts from *Fstl3*+/+ and *Fstl3*−/− mice cultured on 3D-PCL scaffolds were subjected to DCS for 2 h, and the mRNA expression for *Sost* assessed at 4 or 24 h by qRT-PCR. (**b**) Calvarial osteoblasts from *Fstl3*+/+ and *Fstl3*−/− mice were exposed to DCS for 2 h/day and SOST protein expression analyzed following 24 or 48 h by Western blot analysis. (**c**) Digital estimation of the relative intensity of bands in (b). (**d**) Immunohistochemical (A–F) and immunofluorescence (A′–F′) analysis of exercise-dependent SOST expression in the mid-shafts of cortical bones of *Fstl3*+/+ and *Fstl3*−/− mice subjected to daily exercise for 0, 2 or 5 d. (**e**) The relative intensity of SOST expression in cells in a 10^6 sq μm area of femoral cortical bone from *Fstl3*+/+ and *Fstl3*−/− mice showing greater constitutive SOST expression and no change in response to 2 or 5 days of daily exercise, as compared to *Fstl3*+/+ mice. Data in (a, b and c) represent one of 2 separate experiments. Data in (d) represents one out of 5 mice/group and in (e) SEM of 5 mice/group. *indicates $P<0.05$.